DOI: 10.24996/ijs.2024.65.10(SI).24

ISSN: 0067-2904

Calculation of the calibration parameter N_{RSK} of different types of comets

Ruaa Faraj Hanash*, **Salman Zaidan Khalaf**
Department of Astronomy and Space, College of Science, University of Baghdad, Baghdad, Iraq.

Received: 6 /11/2023 Accepted: 10 /9/2024 Published: 15/11/2024

Abstract
This paper gives a dynamic analysis of the recently identified calibration parameter (**N_{RSK}**) in the distance modulus equation for all celestial planets. The parameter **N_{RSK}** has been applied for seven different comets from the Kuiper-Belt region: (1P/Hally, C/2023 E1 (ATLAS), 23P/Brorsen-Metcalf, 20D/Westphal, 12P/Pons-Brooks, 13P/Olbers, and C/2022 P1 (NEOWISE)). This was accomplished by programming data from the Live Sky program from previous years. It is determined that each comet has a distinctive **N_{RSK}** that distinguishes it from other comets and that this parameter does not equal one. According to the data, the seven comets' average **N_{RSK}** is (2.53 for 1P/Hally, 2.561forC/2023 E1 (ATLAS), 2.57 for 23P/Brorsen-Metcalf, 3.07 for 20D/Westphal, 4.11 for 12P/Pons-Brooks, 4.12 for 13P/Olbers, and 3.07 for C/2022 P1 (NEOWISE).

Keywords: comets, apparent magnitude, geocentric, distance modulus

حساب معامل المعايرةN_{RSK}لانواع مختلفة من المذنبات

رؤى فرج حنش * , سلمان زيدان خلف
قسم الفلك والفضاء، كلية العلوم، جامعة بغداد، بغداد، العراق

الخلاصة
تقدم هذه الورقة البحثية تحليلا ديناميكيا لعامل المعايرة(N_{RKS}) التي تم تحديدها مؤخرا في معادلة معامل المسافة لجميع الكواكب السماوية.حيث تم تطبيق هذا العاملN_{RKS} على سبعة مذنبات مختلفة من منطقة حزام كويبر: (1 Hally / P، C / 2023 E1 (ATLAS)، Brorsen-Metcalf / 23P، 20D / Westphal، 12P / Pons-Brooks، 13P / Olbers ، و C / 2022 P1 (NEOWISE)).وتم تحقيق ذلك من خلال برمجة البيانات من برنامج Live Sky من خلال السنوات السابقة. وتم تحديد أن كل مذنب له N_{RKS}خاص به يميزه عن المذنبات الأخرى وأن هذه العامل لا يساوي واحدا. ووفقا للبيانات ، فإن معدلN_{RKS} للمذنبات السبعة هو (1P / Hally = 2.53224، C / 2023 E1 (ATLAS) =2.561602، 23 Brorsen-Metcalf / P=2.577643، 20 Westphal / D=3.074265، 12 / P Pons-Brooks=4.116883، 13Olbers / P ، و C / 2022 P1 (NEOWISE=3.07).

1. Introduction

A heliocentric distance greater than 4 AU was used to observe every comet. Molecular emissions visible above the reflected solar continuum were not detected in most distant comets' spectral measurements.

---

*Email: ruaafarag923@gmail.com

Broadband filters were utilized to investigate the cometary dust environment. Oleksandra Ivanova et al. used dust apparent magnitudes to determine the upper limit of the geometric cross-section of cometary nuclei with radii ranging from 2 km to 28 km [1-5].

A star's brightness is often measured by astronomers using the magnitude system. A star's apparent brightness, m, is its apparent magnitude. The apparent magnitude that a star would have at a distance of 10 parsecs is known as its absolute magnitude M. Parsec is the distance from Earth in ly. A star's apparent magnitude, or brightness as seen from Earth, is determined by the star's distance and intrinsic brightness. A star's absolute magnitude, or M, measures the star's intrinsic brightness. The distance is the only factor influencing the difference between the two, m – M. We refer to this value as the distance modulus [6-10].

The apparent magnitude can be used to estimate the upper limit of the geometric cross-section of a cometary nucleus [11-15].

In 2006, Khalaf showed that the interaction around most of a cometary nucleus is affected by the additional Ions, that the solar wind's plasma has taken up [16]. This causes the average molecular weight to increase and gives rise to various distinctive characteristics in the cometary tail. In front of the IMF, these characteristics were discussed using the explicit and implicit approaches for solving continuity equations. The Beam-Warming approach was the foundation for the implicit method, whereas the explicit method relied on the Lax Finite Difference Scheme [17-20].

In 2008, Khalaf and Selman [21] showed from the interaction between the solar wind and ions comet tail in the presence of MHD (magnetohydrodynamic principles) that temperature changes play a vital role in the energy distribution of cometary tail. The investigation was completed using the explicit Lax-Wendroff method for a three-dimensional spatial simulation model [22-25].

Using MHD magnetohydrodynamic principles, Khalaf determined the temperature of comet ISON's ion tail [26]. The main goal of these equations is to find the ion tail temperature by relating the static and dynamic pressure findings. The findings explained how two different forms of temperature may be inferred. The isotropic temperature, for example, is demonstrated to vary gradually with distance from the cometary nucleus. The second kind, the dynamic temperature, is demonstrated to vary steadily and significantly with cometary nucleus distance [27-30].

In 2016, [31] Khalaf investigated some comet ion features using a CCD camera and the photometry approach, which allowed viewing these images in varying light. The main goal was to get the temperature, velocity, and intensity number distribution from these equations, which give the number of particles per unit volume. The findings accounted for the interaction around the cometary nucleus, primarily influenced by the extra ions supplied to the solar wind's density, the rise in average molecular weight, and many other distinctive features of the cometary tail [32-35].

In 2021, A. Baransky et al. [36] focused on observations of six trans-Neptunian objects (TNOs) at the Kyiv comet station with apparent magnitudes brighter than 20. They calculated the apparent magnitudes in the BVRI (mostly R) bands using the aperture photometry method and found the absolute magnitudes and the color indices in several bands [37-40].

On 26 Feb 2022, Man-To Hui et al. [41], presented a high-resolution observation of distant comet C/2014 UN271 (Bernardinelli-Bernstein) using the Hubble Space Telescope. The nucleus signal was successfully isolated using the nucleus extraction technique, with an apparent V-band magnitude measured to be 21.64 ± 0.11, corresponding to an absolute magnitude of 8.62 ± 0.11 [42-45].

2. Observations

The comet's distance from the earth (Geocentric) and its apparent magnitude for these comets (1P/Hally, C/2023 E1 (ATLAS), 23P/Brorsen-Metcalf, 20D/Westphal, 12P/Pons-Brooks, 13P/Olbers, and C/2022 P1 (NEOWISE)) were collected from the Live Sky program [46] to calculate the $\mathbf{N_{RSK}}$ in using Matlab program, as shown in Table (1-1).

3. Physical model: finding Calibration parameter $\mathbf{N_{RSK}}$

The distance modulus formula is used to determine the distance to an astronomical object, such as a star or galaxy, by measuring its apparent magnitude (m) [47-50]

$$m2 - m1 = 2.5 \log\left(\frac{I1}{I2}\right) \quad \ldots(1)$$

Where m = apparent magnitude for the celestial object,
I = Relative Intensity.
It has been assumed that:

$$m2 - m1 = 2.5\ log((F1/4\pi\ d1^\wedge 2)/\ (F2/4\pi\ d2^\wedge 2)) \quad \ldots(2)$$

Where F=Flux of a celestial object,
d=distance in AU (Astronomical unit)
F_1=F_2 for the same object (comet)

$$m2 - m1 = 5\ \log(d2/d1) \quad \ldots(3)$$

This equation for all objects

$$1 = (m2 - m1)/5\log(d2/d1) \quad ..(4)$$

The left side must be equal to (one) for all measurements of data
From eq. (4), it found that the parameter (the value is one) is a non-constant parameter that is inversely proportional to the distance and directly proportional to the apparent magnitude. This parameter was called **NRKS**, as shown in eq. (5):

$$\mathbf{N_{RSK}} = (m2 - m1)/5\log(d2/d1) \quad \ldots(5)$$

In this study, seven comets have been studied, namely: **(1P/Hally, C/2023 E1 (ATLAS), 23P/Brorsen-Metcalf, 20D/Westphal, 12P/Pons-Brooks, 13P/Olbers,** and **C/2022 P1 (NEOWISE))** from Kuiper-Belt region to find the calibration parameter **(NRSK)** from distance modulus for each of these comets.

By applying eq. (5) and the collected data from Live Sky for the seven comets, $\mathbf{N_{RSK}}$ has been calculated.

4. Results and discussion

N_{RKS} has been calculated according to the Geocentric (AU) and apparent magnitude for the distance modulus equation of the seven comets: (1P/Hally, C/2023 E1 (ATLAS), 23P/Brorsen-Metcalf, 20D/Westphal, 12P/Pons-Brooks, 13P/Olbers, and C/2022 P1 (NEOWISE)) as shown in Table (1-1).

Table 1-1: The seven comets' parameters and average NRKS.

Comet's name	Date	Distance d(AU)	Magnitude (mag)	N_{RKS}	Average N_{RKS}
1P/Hally	26 Jul 2013	34.45	25.39	2.49	2.53
	2 Aug 2014	34.77	25.44	2.29	
	7 Aug 2015	35.05	25.48	2.81	
	24 Jul 2016	35.28	25.52	2.89	
	29 Jul 2017	35.505	25.56	2.80	
	5 Aug 2018	35.68	25.59	2.35	
	10 Aug 2019	35.82	25.61	2.75	
	27 Jul 2020	35.94	25.63	1.84	
	1 Aug 2021	36.03	25.64	2.49	
	8 Aug 2022	34.45	25.39	2.29	
	26 Jul 2023	34.77	25.44		
Comet's name	**Date**	**Distance d(AU)**	**Magnitude (mag)**	**N_{RKS}**	**Average N_{RKS}**
C/2023 E1 (ATLAS)	29 Jul 2013	22.21	32.58	2.60	2.56
	6 Jul 2014	20.95	32.25	2.45	
	13 Jul 2015	19.58	31.89	2.47	
	1 Jul 2016	18.14	31.48	2.57	
	8 Jul 2017	16.56	30.97	2.46	
	15 Jul 2018	14.83	30.38	2.73	
	4 Jul 2019	12.96	29.58	2.48	
	10 Jul 2020	10.83	28.61	2.50	
	15 Jul 2021	8.36	27.2	2.75	
	22 Jul 2022	5.31	24.48		
Comet's name	**Date**	**Distance d(AU)**	**Magnitude (mag)**	**N_{RKS}**	**Average N_{RKS}**
23P/Brorsen-Metchalf	6 Dec 2013	32.38	27.33	3.08	2.57
	11 Dec 2014	32.72	27.4	2.16	
	16 Dec 2015	33.07	27.45	2.63	
	18 Dec 2016	33.36	27.5	3.08	
	13 Dec 2017	33.61	27.55	2.11	
	18 Dec 2018	33.83	27.58	2.61	
	11 Dec 2019	34.009	27.61	3.33	
	15 Dec 2020	34.15	27.64	1.57	
	10 Dec 2021	34.25	27.65		
Comet's name	**Date**	**Distance d(AU)**	**Magnitude (mag)**	**N_{RKS}**	**Average N_{RKS}**
20D/West phal	5 Nov 2013	30.12	30.87	3.33	3.07
	2 Nov 2014	29.83	30.8	2.81	
	30 Oct 2015	29.49	30.73	3.19	
	5 Nov 2016	29.11	30.64	3.16	
	2 Nov 2017	28.69	30.54	3.002	
	30 Oct 2018	28.21	30.43	2.91	
	8 Nov 2019	27.68	30.31	3.04	
	14 Nov 2020	27.10	30.17	3.18	

	11 Nov 2021	26.48	30.01	3.009	
	8 Nov 2022	25.8	29.84	3.08	
	17 Nov 2023	25.04	29.64		
Comet's name	**Date**	**Distance d(AU)**	**Magnitude (mag)**	**N_{RKS}**	**Average N_{RKS}**
12P/Pons-Brooks	11 Dec 2013	22.26	31.7	3.99	4.11
	4 Dec 2014	21.11	31.24	4.14	
	7 Dec 2015	19.86	30.69	4.17	
	11 Dec 2016	18.506	30.05	4.15	
	14 Dec 2017	17.0301	29.3	3.96	
	7 Dec 2018	15.43	28.45	4.18	
	10 Dec 2019	13.64	27.33	4.25	
	2 Dec 2020	11.66	25.88	4.08	
	5 Dec 2021	9.34	23.91	4.08	
	10 Dec 2022	6.51	20.71		
Comet's name	**Date**	**Distance d(AU)**	**Magnitude (mag)**	**N_{RKS}**	**Average N_{RKS}**
13P/Olbers	21 Feb 2013	22.71	31.9	3.85	4.12
	18 Feb 2014	21.65	31.5	4.21	
	27 Feb 2015	20.5	31	4.09	
	26 Feb 2016	19.27	30.45	4.08	
	22 Feb 2017	17.93	29.81	4.06	
	3 Mar 2018	16.47	29.06	4.15	
	28 Feb 2019	14.89	28.15	4.23	
	8 Mar 2020	13.11	26.98	4.06	
	5 Mar 2021	11.15	25.55	4.26	
	16 Mar 2022	8.85	23.41	4.25	
	13 Mar 2023	6.11	19.99		
Comet's name	**Date**	**Distance d(AU)**	**Magnitude (mag)**	**N_{RKS}**	**Average N_{RKS}**
C/2022 P1 (NEOWISE)	4 Jul 2013	20.79	43.47	3.33	3.07
	7 Jul 2014	19.51	42.71	2.81	
	28 Jun 2015	18.15	41.86	3.19	
	30 Jun 2016	16.67	40.87	13.17	
	21 Jun 2017	15.09	39.68	3.00	
	12 Jun 2018	13.35	38.26	2.91	
	3 Jun 2019	11.43	36.39	3.05	
	24 May 2020	9.29	33.85	3.18	
	15 May 2021	6.84	30.04	3.01	
	14 Apr 2022	4.08	23.06	3.05	

Table (1-1), displays the calculated calibration parameter N_{RKS} and the parameters through which it was calculated for the seven comets, which included the distances of that comet from Earth and the apparent magnitudes from 2013 to 2022 or 2023 years, where the distance and the apparent magnitude of each comet were taken in each year. Data were collected for eleven years and the difference between two distances and two apparent magnitudes was calculated for two consecutive years according to the calibration parameter equation. The calibration factor was calculated every two years. Then the rate of the calibration factor was found for each comet. It can be seen that each comet has a unique N_{RSK} that is equivalent to a number and that is not equal to one. This parameter is proportional to the magnitude and is inversely proportional to distance.

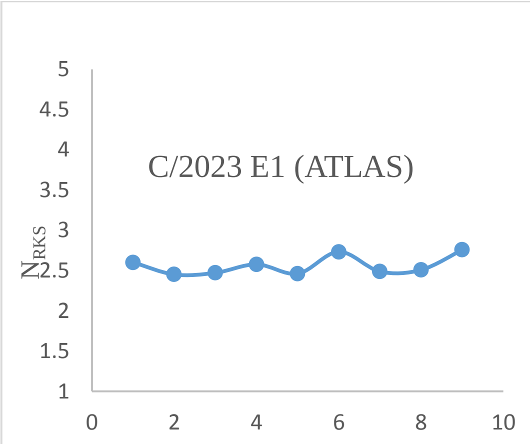

(a)

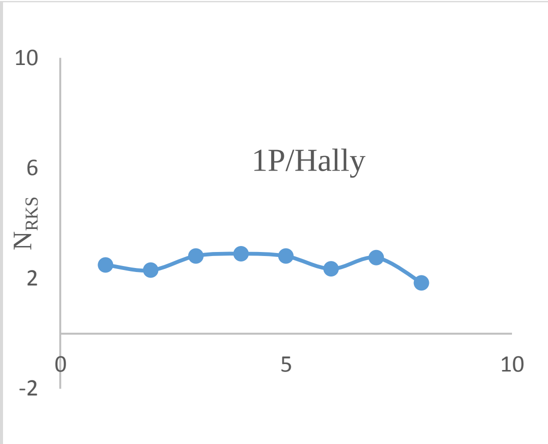

(b)

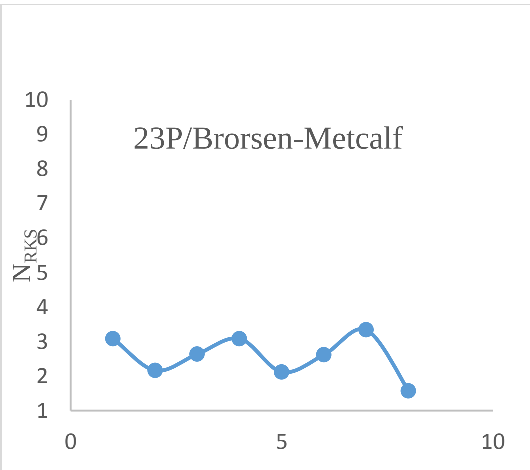

(c)

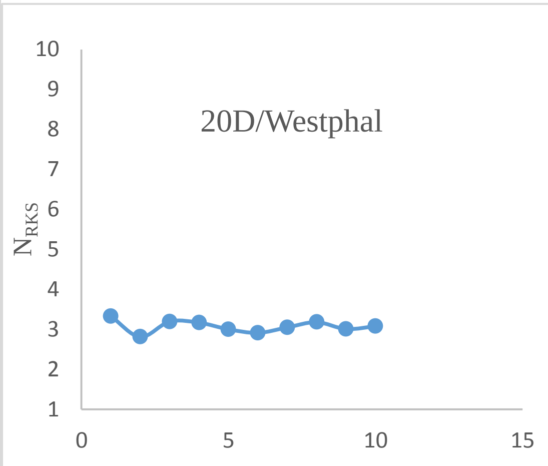

(d)

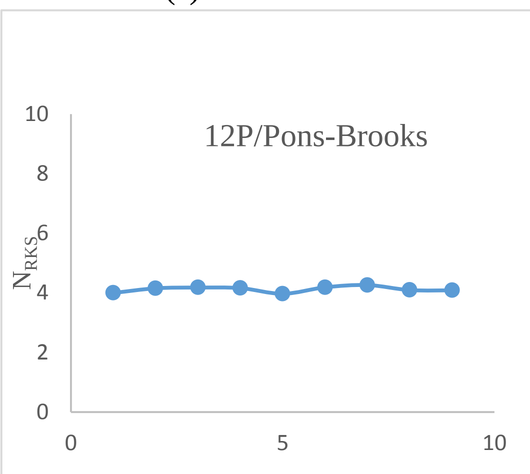

(e)

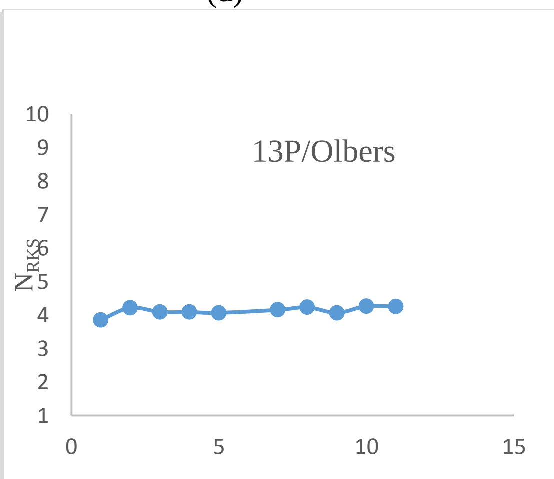

(f)

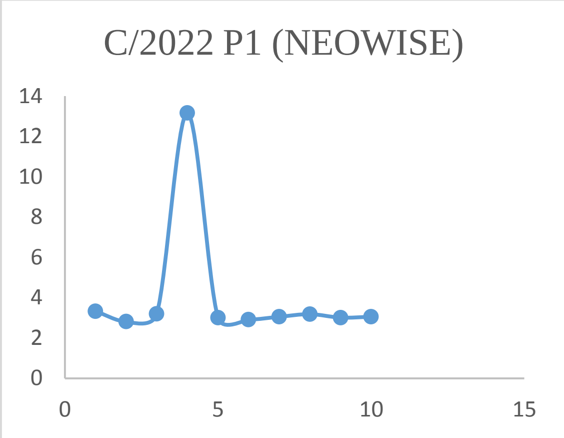

(g)

Figure (1-1): The N_{RKS} for each comet.

Based on the aforementioned Figures, which show the calibration parameter $\mathbf{N_{RSK}}$ for each of the seven comets mentioned above, and where the y-axis and x-axes represent the calibration parameter $\mathbf{N_{RSK}}$ and the number of times the values of the parameter $\mathbf{N_{RSK}}$, it can be concluded that this parameter varies from comet to comet. This variation is caused by the different orbital elements of each comet, even though their faces are in the same region (Kuiper-Belt region). It is attributed to these differences in the size of orbit a (semi-major axis) and the shape of the orbit (eccentricity), as shown in Table (1-2), where these two elements differ in each of the seven comets. This difference affects the calibration parameter $\mathbf{N_{RKS}}$ that was verified from the original equation of the distance factor as in equation (5). It has a constant value for each of them. The average value of $\mathbf{N_{RKS}}$ is shown in Table (1-1).

Table 1-2: represents the orbital elements for the seven comets [46].

The name comet	Semi-major axis (a)	Eccentricity (e)
C/2023 E1 (ATLAS)	19.37 AU	0.946986
1P/Hally	3.51 AU.	0.632
23P/Brorsen-Metcalf	17.07 AU	0.972
20D/Westphal	15.642 AU	0.9198
12P/Pons-Brooks	17.18 AU	0.95460
13P/Olbers	16.90 AU	0.930435
C/2022 P1 (NEOWISE)	18.48 AU	0.913683

The table above (1-2) represents the orbital elements (**Semi-major axis (a)** and **Eccentricity (e)**) of the seven comets for which the calibration parameter $\mathbf{N_{RSK}}$ has been calculated. It was found that the orbital elements of all comets differ from one comet to another, and therefore the different orbital elements, which show the size and shape of the comet's orbit, led to a difference in the value of the $\mathbf{N_{RSK}}$ parameter for each comet.

5. Conclusion

When the calibration parameter NRSK for the distance modulus equation was found and then applied to seven comets, we noted that the average value of **NRSK was** different for all the comets. This difference results from the different orbital snapshots in the shape and size of the orbit of each comet.

In general, we conclude that each comet has its own $\mathbf{N_{RSK}}$. The question on everyone's mind is, what does this operator depend on? Does it depend on the comet's mass, radius, or composition? The answer is unknown but we may know it through future studies.

References

[1] Ivanova, O., Neslušan, L., Krišandová, Z. S., Svoreň, J., Korsun, P., Afanasiev, V., & Andreev, M., "Observations FULL comets C/2007 D1 (LINEAR), C/2007 D3 (LINEAR), C/2010 G3 (WISE), C/2010 S1 (LINEAR), and C/2012 K6 (McNaught) at large heliocentric distances" *Icarus*, vol. 258, pp. 28-36, 2015.

[2] Schmidt-Voigt, M., "Time-dependent MHD simulations for cometary plasmas" *Astronomy and Astrophysics (ISSN 0004-6361)*, vol. 210, no. 1-2, pp. 433-454, 1989.

[3] Kay, C., & Opher, M., "The heliocentric distance is where the deflections and rotations of solar coronal mass ejections occur" *The Astrophysical Journal Letters*, vol. 811, no. 2, pp. L36, 2015.

[4] Hui, M. T., Farnocchia, D., & Micheli, M., "C/2010 U3 (Boattini): A bizarre comet active at record heliocentric distance" *The Astronomical Journal*, vol. 157, no. 4, pp. 162, 2019.

[5] Tancredi, G., Fernández, J. A., Rickman, H., & Licandro, J., "Nuclear magnitudes and the size distribution of Jupiter family comets" *Icarus*, vol. 182, no. 2, pp. 527-549, 2006.

[6] Premovic, P., "The Dimensionality of the Cosmological Distance Modulus Equation" *The General Science Journal*, 2020.

[7] Elyiv, A. A., Melnyk, O. V., Vavilova, I. B., Dobrycheva, D. V., & Karachentseva, V. E., "Machine-learning computation of distance modulus for local galaxies" *Astronomy & Astrophysics*, vol. 635, pp. A124, 2020.

[8] Saviane, I., Momany, Y., Da Costa, G. S., Rich, R. M., & Hibbard, J. E., "A new red giant-based distance modulus of 13.3 Mpc to the antennae galaxies and its consequences" *The Astrophysical Journal*, vol. 678, no. 1, pp. 179, 2008.

[9] Hoffman, Y., Nusser, A., Valade, A., Libeskind, N. I., & Tully, R. B., "From Cosmicflows distance moduli to unbiased distances and peculiar velocities" *Monthly Notices of the Royal Astronomical Society*, vol. 505, no. 3, pp. 3380-3392, 2021.

[10] Blum, J., Gundlach, B., Mühle, S., & Trigo-Rodriguez, J. M., "Comets formed in solar-nebula instabilities!–An experimental and modeling attempt to relate the activity of comets to their formation process" *Icarus*, vol. 235, pp. 156-169, 2014.

[11]Newburn, R. L., Neugebauer, M., & Rahe, J. H., "Comets in the post-Halley era" *Springer Science & Business Media*, vol. 2, 1991.

[12] Hughes, D. W., "The magnitude distribution, perihelion distribution and flux of long-period comets" *Monthly Notices of the Royal Astronomical Society*, vol. 326, no. 2, pp. 515-523, 2001.

[13]Donnison, J. R., "The distribution of cometary magnitudes" *Monthly Notices of the Royal Astronomical Society*, vol. 245, no. 4, pp. 658-658, 1990.

[14] Tancredi, G., Fernández, J. A., Rickman, H., & Licandro, J., "Nuclear magnitudes and the size distribution of Jupiter family comets" *Icarus*, vol. 182, no. 2, pp. 527-549, 2006.

[15] Groussin, O., Attree, N., Brouet, Y., Ciarletti, V., Davidsson, B., Filacchione, G., & Tosi, F., "The thermal, mechanical, structural, and dielectric properties of cometary nuclei after Rosetta" *Space Science Reviews*, vol. 215, pp. 1-51, 2019.

[16]Rubin, M., Altwegg, K., Balsiger, H., Bar-Nun, A., Berthelier, J. J., Briois, C., & Wurz, P., "Krypton isotopes and noble gas abundances in the coma of comet 67P/Churyumov-Gerasimenko" *Science advances*, vol. 4, no. 7, 2018.

[17] Khaleaf, S. Z., &Ibrahim, K, "Expansion velocities of elementary gas in comet Panstarrs above 30000 km from nucleus" *Iraqi Journal of Science*, vol. 61, no. 12, pp. 3417-3433, 2020.

[18]Ezoe Y., Ohashi T., and Mitsuda K., "High-resolution X-ray spectroscopy of astrophysical plasmas with X-ray microcalorimeters" *Reviews of Modern Plasma Physics*, vol. 5, no. 4, pp. 1-43, 2021.

[19]Hanner, M. S., and Bradley, J. P., "Composition and mineralogy of cometary dust" *Comets II*, vol. 555, pp. 564, 2004.

[20] Khalid, A., & Ahmed, Z., "Spectrum Analyzing X-ray Data Image (FITS) Using Ds9 Program" *Journal of Survey in Fisheries Sciences*, vol. 10, no. 3S, pp. 6512-6521, 2023.

[21]Brandt, J. C., Snow, M., Yi, Y., Larson, S. M., Mikuz, H., Petersen, C. C., and Liller, W., "Large Scale Structures In Comet Hale Bopp, Earth, Moon and Planets" vol. 90, pp. 15-33, 2002.

[22]Mozhenkov, E. R., and Vaisberg, O. L., "On the classification of comet plasma tails" *Solar System Research*, vol. 51, pp. 258-270, 2017.

[23]Murawski, K., Boice, D. C., Huebner, W. F., & DeVore, C. R., "Two-dimensional MHD simulations of the solar wind interaction with Comet Halley" *Acta Astronomica*, vol. *48*, pp. 803-817, 1998.

[24] Jalil, M. I., Khalaf, S. Z., & Abbas, Q. A., "Spectroscopy diagnostic for the plasmas of 153P/Ikeya-Zhang and 46P/Wirtanen comets" *AIP Conference Proceedings*, vol. 2372, no. 1, 2021.

[25] Al-Aarajy, K. H. A., & Hassan, Z. H. M., "Land Surface Temperature investigation of Babylon City between (2002-2022) using Remote Sensing and GIS Technique" *Iraqi Journal of Science*, pp. 6686-6693, 2023.

[26] Najm, R. S., Khalaf, S. Z., & Abood, K. I., "Re-Distribution of the Regions of 100 Comets Using a Statistical Method" *Iraqi Journal of Science*, vol. 64, no. 1, pp. 469-479, 2023.

[27]Agúndez, M., Biver, N., Santos-Sanz, P. A., Bockelée-Morvan, D., & Moreno, R., "Molecular observations of comets C/2012 S1 (ISON) and C/2013 R1 (Lovejoy): HNC/HCN ratios and upper limits to PH3" *Astronomy & Astrophysics*, vol. 564, no. L2, 2014.

[28] Velho, L., Frery, A. C., & Gomes, J., "Image processing for computer graphics and vision" *Springer Science & Business Media*, 2009.

[29]Bodewits, D., Christian, D. J., Carter, J. A., Dennerl, K., Ewing, I., Hoekstra, R., & Wolk, S. J., "Cometary charge exchange diagnostics in UV and X-ray" *Astronomische Nachrichten*, vol. 333, no. 4, pp. 335-340, 2012.

[30] Möhlmann, D., Seidensticker, K. J., Fischer, H. H., Faber, C., Flandes, A., Knapmeyer, M., & Arnold, W., "Compressive strength and elastic modulus at Agilkia on comet 67P/Churyumov-Gerasimenko derived from the SESAME/CASSE touchdown signals" *Icarus*, vol. 303, pp. 251-264, 2018.

[31]Lang, K. R., "The life and death of stars", Printed in Singapore by KHL. Printing Co., pp.112-113, 2013.

[32]Lisse, C. M., Fernández, Y. R., Kundu, A., A'Hearn, M. F., Dayal, A., Deutsch, L. K., & Hoffmann, W. F., "The nucleus of comet Hyakutake (C/1996 B2)" *Icarus*, vol. 140, no. 1, pp. 189-204, 1999.

[33] Schleicher, D. G., & Osip, D. J., "Long-and short-term photometric behavior of comet Hyakutake (1996 B2)" *Icarus*, vol. 159, no. 1, pp. 210-233, 2002.

[34]Combi, M. R., Cochran, A. L., Cochran, W. D., Lambert, D. L., & Johns-Krull, C. M., "Observation and analysis of high-resolution optical line profiles in comet Hyakutake (C/1996 B2)" *The Astrophysical Journal*, vol. 512, no. 2, pp. 961, 1999.

[35] Biele, J., Vincent, J. B., & Knollenberg, J., "Mechanical properties of cometary surfaces" *Universe*, vol. 8, no. 9, pp. 487, 2022.

[36]Baransky, A., Lukina, O., & Borysenko, S., "Astrometric and photometric observations of six brightest trans-Neptunian objects at the Kyiv comet station" *arXiv preprint arXiv: 2107.02771*, 2021.

[37] Kokhirova, G. I., Ivanova, O. V., Rakhmatullaeva, F. D., Buriev, A. M., & Khamroev, U. K., "Astrometric and photometric observations of comet 29P/Schwassmann-Wachmann 1at the Sanglokh international astronomical observatory" *Planetary and Space Science*, vol. 181, no. 104794, 2020.

[38] Lowry, S. C., & Fitzsimmons, A., "CCD photometry of distant comets II" *Astronomy & Astrophysics*, vol. 365, no. 2, pp. 204-213, 2001.

[39] Roemer, E., "Luminosity and astrometry of comets: A review" In *International Astronomical Union Colloquium*, Cambridge University Press, vol. 25, no. Part1, pp. 380-409, 1976.

[40] Abdullah, S. A., Abbas, K. H., Harif, A. H., Alaa, R. F., & Hiba, S., "Sustainable Urban Distribution of Educational Institutions and Population Density in Baghdad City Using Remote Sensing Techniques" In *IOP Conference Series: Earth and Environmental Science*, vol. 1202, no. 1, pp. 012015, 2023.

[41]Hui, M. T., Jewitt, D., Yu, L. L., & Mutchler, M. J. "Hubble Space Telescope Detection of the Nucleus of Comet C/2014 UN271 (Bernardinelli–Bernstein)" *The Astrophysical Journal Letters*, vol. 929, no. L12, 2022.

[42] Jensen, J. W., "Supernovae light curves: An Argument for a new distance modulus" ArXiv *preprint astro-ph/0404207*, 2004.

[43] Falkner, D. E., "Measuring Cosmic Distances" *In Stories of Astronomers and Their Stars*, Springer, Cham, pp. 209-218, 2021.

[44] Wu, T., Li, Y., & Hekker, S., "Asteroseismic Study on Cluster Distance Moduli for RGB Stars in NGC 6791 and NGC 6819" *arXiv preprint arXiv:1403.5838*, 2014.

[45] Watson, D., Denney, K. D., Vestergaard, M., & Davis, T. M., "A new cosmological distance measure using active galactic nuclei" *The Astrophysical Journal Letters*, vol. 740, no. 2, pp. L49, 2011.

[46]https://theskylive.com.[Accessed: 2- August. – 2023].

[47]Hughes, D. W., & Daniels, P. A., "The magnitude distribution of comets" *Monthly Notices of the Royal Astronomical Society*, vol, 191, no. 3, pp. 511-520, 1980.

[48] Zanetti, L., "Sparse formulae for the distance modulus in cosmology" *arXiv preprint arXiv: 2107.12140*, 2021.

[49] Elyiv, A. A., Melnyk, O. V., Vavilova, I. B., Dobrycheva, D. V., & Karachentseva, V. E., "Machine-learning computation of distance modulus for local galaxies" *Astronomy & Astrophysics*, vol. 635, pp. A124, 2020.

[50] Wu, T., Li, Y., & Hekker, S., "Asteroseismic study on cluster distance moduli for red giant branch stars in NGC 6791 and NGC 6819" *The Astrophysical Journal*, vol. 786, no. 1, pp. 10, 2014.